Published in final edited form as:
Biomaterials. 2008 December ; 29(36): 4775–4782. doi:10.1016/j.biomaterials.2008.08.022.

COLLAGEN FIBER ALIGNMENT AND BIAXIAL MECHANICAL BEHAVIOR OF PORCINE URINARY BLADDER DERIVED EXTRACELLULAR MATRIX

Thomas W. Gilbert[1], **Silvia Wognum**[2], **Erinn M. Joyce**[2], **Donald O. Freytes**[1], **Michael S. Sacks**[2], and **Stephen F. Badylak**[1]

1*McGowan Institute for Regenerative Medicine, Department of Surgery, University of Pittsburgh, Pittsburgh, PA*

2*Engineered Tissue Mechanics and Mechanobiology Laboratory, Department of Bioengineering, University of Pittsburgh, Pittsburgh, PA*

Abstract

The collagen fiber alignment and biomechanical behavior of naturally occurring extracellular matrix (ECM) scaffolds are important considerations for the design of medical devices from these materials. Both should be considered in order to produce a device to meet tissue specific mechanical requirements (e.g., tendon vs. urinary bladder), and could ultimately affect the remodeling response *in vivo*. The present study evaluated the collagen fiber alignment and biaxial mechanical behavior of ECM scaffold material harvested from porcine urinary bladder tunica mucosa and basement membrane (together referred to as urinary bladder matrix (UBM)) and ECM harvested from urinary bladder submucosa (UBS). Since the preparation of UBM allows for control of the direction of delamination, the effect of the delamination method on the mechanical behavior of UBM was determined by delaminating the submucosa and other abluminal layers by scraping along the longitudinal axis of the bladder (apex to neck) (UBML) or along the circumferential direction (UBMC). The processing of UBS does not allow for similar directional control. UBML and UBS had similar collagen fiber distributions, with a preferred collagen fiber alignment along the longitudinal direction. UBMC showed a more homogenous collagen fiber orientation. All samples showed a stiffer mechanical behavior in the longitudinal direction. Despite similar collagen fiber distributions, UBML and UBS showed quite different mechanical behavior for the applied loading patterns with UBS showing a much more pronounced toe region. The mechanical behavior for UBMC in both directions was similar to the mechanical behavior of UBML. There are distinct differences in the mechanical behavior of different layers of ECM from the porcine urinary bladder, and the processing methods can substantially alter the mechanical behavior observed.

Introduction

The relationship between the biomechanical behavior of naturally occurring extracellular matrix (ECM) scaffolds and the remodeling of these scaffolds *in vivo* is not fully understood. The ability of a scaffold at the time of implantation to accommodate at least passive physiologic

Corresponding author: Stephen F. Badylak, McGowan Institute for Regenerative Medicine, University of Pittsburgh, 100 Technology Drive, Suite 200, Pittsburgh, PA 15219, P: (412) 235-5144, F: (412) 235-5110, badylaks@upmc.edu.

loading is essential for a clinically acceptable outcome. Ideally, a scaffold would closely mimic the mechanical behavior of the tissue that it is intended to replace [1]. The mechanical properties of an ECM scaffold are largely a function of the collagen fiber alignment and kinematics of the material, which in turn regulate the behavior of cells that migrate to the site of ECM remodeling. Thus, the three dimensional organization of new host tissue is influenced by the collagen fiber architecture of the original scaffold. An understanding of the collagen fiber alignment and biaxial mechanical behavior of ECM scaffold materials harvested from different tissue sites should logically improve the ability to predict their suitability for various tissue replacement applications. In addition, it is also necessary to understand how the manufacturing steps used to produce an ECM scaffold affect the collagen fiber architecture and mechanical behavior.

The most extensively studied ECM scaffold with regard to mechanical behavior is porcine small intestinal submucosa (SIS-ECM). SIS-ECM has been shown to consist primarily of two populations of collagen fibers with centroids that are shifted approximately 30° from the longitudinal axis of the small intestine that together create a preferred fiber direction along the longitudinal axis of the small intestine [2]. The fibers have been shown to have considerable motility, showing global fiber rotation at low strains when stretched along the preferred fiber direction, and continued individual rotation and stretch with increasing levels of strain [3,4]. This preferred fiber alignment corresponded to transverse anisotropic behavior under biaxial mechanical loading [2].

ECM scaffold materials derived from the urinary bladder have become widely studied recently for a number of applications, including repair of the urinary bladder, esophagus, and myocardium [5–12]. The current study examines the collagen fiber alignment and biaxial mechanical behavior of two ECM scaffolds derived from the porcine urinary bladder, namely urinary bladder matrix (UBM) and urinary bladder submucosa (UBS). These scaffolds are derived from adjacent layers of the same tissue and have both been used in pre-clinical regenerative medicine applications. In addition, the effect of mechanical delamination of the layers of the urinary bladder during processing, in particular the direction of applied force, upon the collagen fiber alignment is described.

Methods

ECM device preparation

The preparation of UBM and UBS has been previously described [6,7,13]. Nine porcine urinary bladders were harvested from market weight pigs (approximately 110–130 kg) immediately after sacrifice. Residual external connective tissues, including adipose tissue, were trimmed and all residual urine was removed by repeated washes with tap water. The urothelial layer was removed by soaking of the material in 1 N saline.

Urinary Bladder Matrix (UBM)—For the urinary bladders used to prepare UBM (n=6), the tunica serosa, tunica muscularis externa, tunica submucosa, and most of the muscularis mucosa were mechanically delaminated from the bladder tissue. The remaining basement membrane of the tunica epithelialis mucosa and the subjacent tunica propria were collectively termed UBM. Attention was paid to the direction of delamination such that three sheets of UBM were prepared by delaminating the tissue from the apex to the neck of the bladder (i.e., longitudinally) and three bladders were prepared by circumferential delamination.

Urinary Bladder Submucosa (UBS)—For the urinary bladders used to prepare UBS (n=3), the tunica serosa and tunica muscularis externa were mechanically delaminated from the bladder tissue by blunt scraping upon a flat surface. The process of separation of the layers made it impossible to maintain a preferred direction of scraping. The remaining tissue was then

turned over and the luminal layers consisting of the basement membrane of the tunica epithelialis mucosa and the subjacent tunica propria were mechanically separated leaving only the tunica submucosa and portions of the muscularis mucosa.

All specimens were decellularized and disinfected by immersion in 0.1% (v/v) peracetic acid (PAA) (σ), 4% (v/v) ethanol, and 96% (v/v) deionized water for 2 h. The material was then washed twice for 15 min with PBS (pH = 7.4) and twice for 15 min with deionized water [7, 14].

Collagen Fiber Alignment

The full sheets of UBM and UBS were optically cleared by immersion in graded solutions of glycerol to 100%. The sheets were then mounted flat in a 20 cm × 25 cm glass well consisting of panes of glass sealed with silicone caulk. The glass well was then filled with 100% glycerol for assessment of the collagen fiber architecture by small angle light scattering (SALS) [15]. Briefly, the SALS system consisted of a 4 MW HeNe (632.8 nm) continuous unpolarized wave laser. As the laser passed through the tissue, it was scattered onto a white plastic screen. The resulting scattering pattern was recorded with a CCD camera system and was analyzed using custom software. The scattering pattern, I(θ), represented the angular distribution of collagen fibers within the light beam envelope [15]. The specimen was mounted on an X-Y stage that allowed the entire specimen to be analyzed by successive passes across the tissue. Due to the size of samples, a beam diameter of 750 μm was used with a step size of 1.5 mm between measurements.

From each scattering pattern, the preferred fiber orientation and an orientation index (OI) were calculated. The OI has been defined as an angle about the preferred fiber direction that contained 50% of all fibers [15]. In the present study, a normalized orientation index (NOI) was defined as NOI = (90° - OI)/90° × 100% [3]. An NOI of 100% indicated that the collagen fibers in the tissue were perfectly aligned, and an NOI of 0% indicated random fiber alignment.

Biaxial Mechanical Testing

A detailed description of the biaxial testing device has been presented previously [16,17]. The specimens were mounted on the device with 8 equal length loops of 000 nylon suture attached to stainless steel surgical staples (2 loops per side). All tests were performed with hydrated (never lyophilized) specimens immersed in PBS at room temperature. The test protocol consisted of load controlled biaxial testing with the specimen stretched to a maximum load (P) of 100g, with load ratios of P_L:P_C = 1.0:1.0, 1.0:0.1, 1.0:0.5, 1.0:0.75: 1.0:1.0, 0.75:1.0, 0.5:1.0, 0.1:1.0. 1.0:1.0. The initial and final equibiaxial tests were conducted to verify that the tissue was not damaged by testing. The strain was monitored during the test using a CCD camera to visualize 4 graphite markers fixed to the specimen in a 5 mm × 5 mm square. Each loading protocol was applied 10 times to precondition the specimen and the 10^{th} cycle was used for analysis.

From the marker positions, the deformation gradient tensor **F** was calculated at each data point [3,18]. The components of the in-plane Green strain tensor **E** were calculated using $\mathbf{E} = \frac{1}{2}(\mathbf{F}^T\mathbf{F} - 1)$. The shear components of **F** were negligible in all test specimens, so the in-plane components of **E** were determined using $E_C = \frac{1}{2}(\lambda_C^2 - 1)$ and $E_L = \frac{1}{2}(\lambda_L^2 - 1)$. The first Piola-Kirchhoff stress tensor **P** was calculated from the measured loads and the initial specimen dimensions. The second Piola-Kirchhoff stress tensor **S** was determined using $\mathbf{S} = \mathbf{P}\mathbf{F}^{-T}$.

Biaxial Mechanical Response

The pseudo-elastic response of UBM and UBS was determined in a protocol dependent manner using a previous by described methodology [19,20]. Briefly, the **S**–**E** data for each specimen axes were individually fit to the following response functions:

$$S_{11}=\frac{c_{10}}{2}\left(2c_{11}E_{11}+2c_{13}E_{22}+2c_{14}E_{11}E_{22}+c_{15}E_{22}^2+2c_{16}E_{11}E_{22}^2+4c_{17}E_{11}^3\right)\exp A_1$$

$$S_{22}=\frac{c_{20}}{2}\left(2c_{22}E_{22}+2c_{23}E_{11}+2c_{25}E_{22}E_{11}+c_{24}E_{11}^2+2c_{26}E_{11}^2E_{22}+4c_{28}E_{22}^3\right)\exp A_2$$

where:

$$A_1=c_{11}E_{11}^2+c_{12}E_{22}^2+2c_{13}E_{11}E_{22}+c_{14}E_{11}^2E_{22}+c_{15}E_{22}^2E_{11}+c_{16}E_{11}^2E_{22}^2+c_{17}E_{11}^4+c_{18}E_{22}^4$$

$$A_2=c_{21}E_{11}^2+c_{22}E_{22}^2+2c_{23}E_{11}E_{22}+c_{24}E_{11}^2E_{22}+c_{25}E_{22}^2E_{11}+c_{26}E_{11}^2E_{22}^2+c_{27}E_{11}^4+c_{28}E_{22}^4$$

and c_{ij} are fitted parameters and E_{ii} were the components of Green strain tensor. These response functions were independently fit to all stress–strain data using the nonlinear regression in MathCAD software. The resulting response surfaces were used as a qualitative guide in the choice of W by plotting contours of constant stress for S_C and S_L. For a perfectly isotropic material, such contours would display symmetry about the $y = x$-axis, while asymmetry would indicate the presence of anisotropy.

Statistical Analyses

Comparative statistics were used for comparisons of the distributions of centroids by creating histograms of the number of scan regions with a centroid within a prescribed range of θ. A student T-test was used to compare the NOI within the prescribed range of θ. A two-way ANOVA (scaffold and direction) with Tukey's post-hoc analysis was performed to determine statistical differences between the modulus and the stretch in the toe region (stretch to reach 100 kPa).

Results

Analysis of the collagen fiber alignment showed that in general, UBM and UBS both had a preferred fiber direction along the longitudinal direction of the bladder (i.e., oriented from the apex to the neck). However, the degree of this preference varied primarily based upon the method of production. For UBM scraped longitudinally (UBML) and UBS, there was a pronounced preferred fiber alignment towards the longitudinal direction (Fig. 1, Fig. 2A, Fig 3A). The percentage of collagen fiber alignment measurements within 20° of the longitudinal axis of the bladder was 76.9% for UBM scraped longitudinally and 68.2% for UBS. For UBM scraped circumferentially (UBMC), the fiber alignment was much more homogenous, with only a slight preference towards an angle approximately 15° from the longitudinal direction (24.1% of observations between −30° and 0°) (Fig. 1and Fig. 4A). The average NOI for the tissues ranged from 46% to 54% depending on the θ-range of interest. The NOI for UBMC was statistically less than that for UBML and UBS within the θ range of −20° to 20° ($p < 0.05$).

Biaxial mechanical testing of the UBML, UBMC, and UBS showed mechanical behavior that was consistent with the collagen fiber alignment results. Equibiaxial testing of UBM and UBS showed transverse anisotropy, with a significantly stiffer modulus along the longitudinal axis of the tissue and the toe region was significantly longer in the circumferential direction ($p < 0.05$) (Table 1) (Fig. 2B, 3B, and 4B). Generally, the UBML showed the greatest degree of transverse anisotropy with a modulus that was five times greater in the longitudinal direction than in the circumferential direction, compared with an approximately two fold difference for UBS and UBMC. The modulus in the longitudinal direction was not significantly different between UBML and UBMC, but the modulus in the longitudinal direction for UBS was significantly less than UBML and UBMC ($p < 0.05$). In the circumferential direction, UBMC

had the greatest modulus ($p < 0.05$). The toe region was significantly longer in the longitudinal direction for UBS as compared to UBML and UBMC ($p < 0.05$), and there was no difference between UBML and UBMC. UBMC had the shortest toe region of all groups in the circumferential direction ($p < 0.05$). The lower stresses in UBS were due to a greater thickness for UBS (130 ± 23 μm) compared to UBM (85 ± 5 μm).

The nonequibiaxial mechanical testing data showed mechanical coupling between the two transverse loading directions for UBML (Fig. 2C), UBS (Fig. 3C), and to a lesser extent UBMC (Fig. 4C). For UBML and UBS, mechanical coupling was observed with relatively uniform changes in the mechanical behavior in direction of maximum load for a change in the loading in the transverse direction. For UBMC, asymmetric mechanical coupling was observed since there were changes in the mechanical behavior in the longitudinal direction associated with changes in the loading in the circumferential direction, but no changes were observed in the mechanical behavior in the circumferential direction for changes in the loading in the longitudinal direction. Passive tissue shortening was observed for the longitudinal direction and the circumferential direction for load ratios of 0.1:1.0 and 1.0:0.1, respectively. The passive tissue shortening led to greater increases in stress value for the longitudinal direction than was observed for the circumferential direction.\

From the response functions for each specimen, two-dimensional contour plots were generated over the realized experimental strain plane to allow direct examination of material symmetries. This allowed evaluation of material class and degree of anisotropy directly from the experimental data. The existence and direction of marked anisotropy were apparent in the UBML and UBS tissue, with a distinct bias toward the longitudinal direction (apex-neck). In contrast, the UBMC response was less anisotropic, with only a slight bias toward the longitudinal direction, which corresponded to the collagen fiber alignment. (Fig. 2–4 D and E).

Discussion

The present study showed that differences existed in the collagen fiber alignment and biaxial biomechanical behavior of ECM scaffold materials derived from the porcine urinary bladder depending upon the layer from which the scaffold was obtained and the processing to which the scaffold was subjected. In general, the porcine urinary bladder was shown to have preferred collagen fiber alignment and a greater modulus in the longitudinal axis of the tissue. This collagen fiber alignment was consistent with previous findings in the rat bladder that showed longitudinal alignment of the smooth muscle and an increased stiffness of the full thickness bladder in the longitudinal direction [21,22].

UBML and UBS showed very similar collagen fiber distributions, but the biomechanical behavior was quite different with a longer toe region and lower modulus observed for UBS over the range of loads applied. This result was in contrast to a previous study in which multilaminate devices of UBM and UBS were subjected to ball burst testing [13]. In that case, the UBS multilaminate scaffold was significantly stronger than the UBM multilaminate scaffolds. The preparation of a multilaminate scaffold also changed the mechanical properties of the scaffold by altering the fibrous structure of each individual layer [13]. The differences observed in the present study may have been a result of aggressive scraping that was done to remove the tunica submucosa, tunica muscularis externa, and tunica serosa from the UBM that may have reoriented and reduced the crimping of collagen within the tissue. At greater loads, it is possible that UBS would still reach a greater modulus and ultimate strength than UBM.

The comparisons between UBML and UBMC showed that the methods of preparation have an effect upon the resulting collagen fiber alignment and biomechanical behavior of the tissue.

UBML and UBMC showed very different collagen fiber distributions, UBML showing high longitudinal alignment and UBMC showing a more homogeneous collagen fiber distribution. However, the longitudinal biomechanical properties for UBML and UBMC were very similar for the loading conditions applied, and the circumferential biomechanical behavior for UBMC approached the longitudinal biomechanical behavior. The process of scraping the tissue circumferentially rotated a substantial population of collagen fibers from the longitudinal direction towards the circumferential direction, and the results clearly showed that those fibers retained the new orientation. Moreover, the fact that the longitudinal biomechanical behavior did not substantially change suggested that there was a population of collagen “struts” that were relatively fixed in the longitudinal direction and served to limit the longitudinal elongation of the bladder.

The biomechanical behavior and/or collagen fiber alignment were evaluated for a number of other ECM scaffolds in previous studies. The results for the present study compared well with the results of similar analyses performed with SIS-ECM [2]. SIS-ECM also possessed a preferred collagen fiber alignment along the longitudinal axis of the tissue, and was composed of two populations of collagen fibers that were each offset by approximately 30° from the longitudinal axis. No evidence of a bimodal collagen distribution was observed for ECM derived from UBM in the present study, but this may have been due to the relatively large beam diameter used in this study. Previous studies with SIS-ECM have also shown a substantial degree of collagen fiber motility in response to uniaxial loading and strip biaxial loading, especially in the hydrated state [3,4]. SIS-ECM is typically delaminated by applying pressure along the longitudinal axis of the intestine, so processing may have contributed to the relatively uniform collagen fiber alignment. This explanation would support the concept that circumferential scraping of the UBM led to large fiber rotations.

In contrast to SIS-ECM and the urinary bladder ECM studied in the present study, it was recently found that cholecyst-derived ECM (CEM) possessed a preferred collagen fiber orientation offset by approximately 65° from the longitudinal axis (i.e., from the neck to the fundus) [23]. Using the preferred fiber direction as the principal direction for mechanical testing [23], the biomechanical behavior for CEM was similar to UBMC in terms of the stress-strain relationship and the weakly anisotropic behavior. There was no specific mention of whether the direction of delamination was controlled in the preparation of CEM.

The results of the present study have direct implications for the fabrication of medical devices from ECM scaffolds. It has been reported that the mechanical behavior of SIS-ECM is dependent upon the segment of the small intestine from which the SIS is harvested [24]. It is possible that these differences may be a function not only of biologic variability of the tissue, but also process variability. It is therefore important to monitor the direction and magnitude of pressure that was applied to the tissue. These findings could also factor into the design of an ECM device. A recent study compared the mechanical behavior of several commercially available ECM derived devices indicated for rotator cuff repair to determine how they compared to the mechanical behavior of the infraspinatus tendon [1]. In all cases, the mechanical behavior of the scaffold was inferior to that of the tendon, with a lower stiffness and strength. One of the devices evaluated was Restore (DePuy Orthopaedics, Warsaw, IN), a device composed of 10 layers of SIS-ECM that is configured such that 2 layers of ECM are aligned every 72° to give the device an isotropic mechanical behavior. Based on the present results, it is possible that an ECM scaffold could be processed in such a way that it may more closely mimic the biomechanical properties of the tissue the scaffold is intended to replace. Using UBM as an example, for designing a device for tendon repair, the material could be scraped longitudinally and then laminated such that the longitudinal axis of the bladder is aligned for all of the layers, providing a transversely anisotropic material similar to a tendon. By prestretching the scaffold prior to lamination, the degree of transverse anisotropy could be

increased [3]. Conversely, for repair of body wall, the UBM could be scraped circumferentially and laminated with random orientation of the sheets to provide an isotropic mechanical behavior. Additional study is necessary to verify these predictions.

It should be noted that the results from the present study are only applicable to the scaffolds prior to implantation. In the absence of chemical crosslinking, an ECM scaffold begins to be degraded immediately by the host, altering their mechanical properties during the process of remodeling. Previous studies have shown that ECM scaffolds are completely degraded within 60–90 days [25,26], and the degradation products are small bioactive peptides that have chemotactic, bacteriostatic, and mitotic properties [27–30]. The chemotactic peptides may be responsible for the recruitment of bone marrow derived progenitor cells that participate in the remodeling by differentiating into site specific cells in response to mechanical and biochemical cues [31–33]. Since the mechanical environment is defined by the collagen fiber architecture and kinematics, the changes in these properties of the scaffold are an important topic of future study.

A limitation of the present study is that the specimens were only subjected to subfailure biaxial testing. Uniaxial testing to failure may have provided additional information about whether the increased collagen fiber alignment would result in changes in tensile properties of the tissue. Comparison of these results to previous work is confounded by the lack of control for orientation of the test articles relative to the anatomic orientation of the urinary bladder [34–36]. The biaxial testing used in the present study was selected to provide a broad understanding of the material behavior within physiologically relevant ranges of load and strain. In addition, the data collected in this study will be useful in the development of structural constitutive models of the ECM of the urinary bladder [37], which could be useful for predicting the remodeling response of a scaffold *in vivo* or optimal mechanical loading regimens *in vitro* [38–40].

Conclusions

ECM derived from different layers of the porcine urinary bladder, namely the tunica submucosa (UBS) and the tunica mucosa and basement membrane (UBM) show differences in their biaxial mechanical behavior. Both ECM materials possess a preferred fiber alignment along the longitudinal axis of the bladder, but the distribution of the collagen alignment is substantially altered during processing, making the material less transversely anisotropic. The results of this study may have implications for the production of medical devices for repair of tissues with highly specific mechanical requirements.

References

1. Derwin KA, Baker AR, Spragg RK, Leigh DR, Iannotti JP. Commercial extracellular matrix scaffolds for rotator cuff tendon repair. Biomechanical, biochemical, and cellular properties. J Bone Joint Surg Am 2006 Dec;88(12):2665–2672. [PubMed: 17142417]
2. Sacks MS, Gloeckner DC. Quantification of the fiber architecture and biaxial mechanical behavior of porcine intestinal submucosa. J Biomed Mater Res 1999 Jul;46(1):1–10. [PubMed: 10357130]
3. Gilbert TW, Sacks MS, Grashow JS, Woo SL-Y, Badylak SF, Chancellor MB. Fiber kinematics of small intestinal submucosa under biaxial and uniaxial stretch. J Biomech Eng 2006 Dec;128(6):890–898. [PubMed: 17154691]
4. Gloeckner DC, Sacks MS, Billiar KL, Bachrach N. Mechanical evaluation and design of a multilayered collagenous repair biomaterial. J Biomed Mater Res 2000 Nov;52(2):365–373. [PubMed: 10951377]
5. Atala A, Bauer SB, Soker S, Yoo JJ, Retik AB. Tissue-engineered autologous bladders for patients needing cystoplasty. Lancet 2006 Apr 15;367(9518):1241–1246. [PubMed: 16631879]
6. Badylak SF, Meurling S, Chen M, Spievack A, Simmons-Byrd A. Resorbable bioscaffold for esophageal repair in a dog model. J Pediatr Surg 2000 Jul;35(7):1097–1103. [PubMed: 10917304]

7. Badylak SF, Vorp DA, Spievack AR, Simmons-Byrd A, Hanke J, Freytes DO, et al. Esophageal reconstruction with ECM and muscle tissue in a dog model. J Surg Res 2005 Sep;128(1):87–97. [PubMed: 15922361]
8. Bolland F, Korossis S, Wilshaw SP, Ingham E, Fisher J, Kearney JN, et al. Development and characterisation of a full-thickness acellular porcine bladder matrix for tissue engineering. Biomaterials 2007 Feb;28(6):1061–1070. [PubMed: 17092557]
9. Brown AL, Farhat W, Merguerian PA, Wilson GJ, Khoury AE, Woodhouse KA. 22 week assessment of bladder acellular matrix as a bladder augmentation material in a porcine model. Biomaterials 2002 May;23(10):2179–2190. [PubMed: 11962659]
10. Kochupura PV, Azeloglu EU, Kelly DJ, Doronin SV, Badylak SF, Krukenkamp IB, et al. Tissue-engineered myocardial patch derived from extracellular matrix provides regional mechanical function. Circulation 2005 Aug 30;112(9 Suppl):I144–I149. [PubMed: 16159807]
11. Nieponice A, Gilbert TW, Badylak SF. Reinforcement of esophageal anastomoses with an extracellular matrix scaffold in a canine model. Ann Thorac Surg 2006 Dec;82(6):2050–2058. [PubMed: 17126109]
12. Robinson KA, Li J, Mathison M, Redkar A, Cui J, Chronos NA, et al. Extracellular matrix scaffold for cardiac repair. Circulation 2005 Aug 30;112(9 Suppl):I135–I143. [PubMed: 16159805]
13. Freytes DO, Badylak SF, Webster TJ, Geddes LA, Rundell AE. Biaxial strength of multilaminated extracellular matrix scaffolds. Biomaterials 2004 May;25(12):2353–2361. [PubMed: 14741600]
14. Brown B, Lindberg K, Reing J, Stolz DB, Badylak SF. The basement membrane component of biologic scaffolds derived from extracellular matrix. Tissue Eng 2006 Mar;12(3):519–526. [PubMed: 16579685]
15. Sacks MS, Smith DB, Hiester ED. A small angle light scattering device for planar connective tissue microstructural analysis. Ann Biomed Eng 1997;25(4):678–689. [PubMed: 9236980]
16. Sacks MS, Chuong CJ. Orthotropic mechanical properties of chemically treated bovine pericardium. Ann Biomed Eng 1998;26(5):892–902. [PubMed: 9779962]
17. Sacks MS. A method for planar biaxial mechanical testing that includes in-plane shear. J Biomech Eng 1999;121(5):551–555. [PubMed: 10529924]
18. Sacks MS. Biaxial mechanical evaluation of planar biological materials. Journal of Elasticity 2000;61:199–246.
19. Sun W, Sacks MS, Sellaro TL, Slaughter WS, Scott MJ. Biaxial mechanical response of bioprosthetic heart valve biomaterials to high in-plane shear. J Biomech Eng 2003 Jun;125(3):372–380. [PubMed: 12929242]
20. Vande Geest JP, Sacks MS, Vorp DA. Age dependency of the biaxial biomechanical behavior of human abdominal aorta. J Biomech Eng 2004 Dec;126(6):815–822. [PubMed: 15796340]
21. Gloeckner DC, Sacks MS, Fraser MO, Somogyi GT, de Groat WC, Chancellor MB. Passive biaxial mechanical properties of the rat bladder wall after spinal cord injury. J Urol 2002 May;167(5):2247–2252. [PubMed: 11956487]
22. Nagatomi J, Toosi KK, Grashow JS, Chancellor MB, Sacks MS. Quantification of bladder smooth muscle orientation in normal and spinal cord injured rats. Ann Biomed Eng 2005 Aug;33(8):1078–1089. [PubMed: 16133916]
23. Coburn JC, Brody S, Billiar KL, Pandit A. Biaxial mechanical evaluation of cholecyst-derived extracellular matrix: A weakly anisotropic potential tissue engineered biomaterial. J Biomed Mater Res A 2007 Apr;81(1):250–256. [PubMed: 17269134]
24. Raghavan D, Kropp BP, Lin HK, Zhang Y, Cowan R, Madihally SV. Physical characteristics of small intestinal submucosa scaffolds are location-dependent. J Biomed Mater Res A 2005 Apr 1;73(1):90–96. [PubMed: 15693016]
25. Gilbert TW, Stewart-Akers AM, Simmons-Byrd A, Badylak SF. Degradation and remodeling of small intestinal submucosa in canine Achilles tendon repair. J Bone Joint Surg Am 2007 Mar;89(3):621–630. [PubMed: 17332112]
26. Record RD, Hillegonds D, Simmons C, Tullius R, Rickey FA, Elmore D, et al. *In vivo* degradation of ^{14}C-labeled small intestinal submucosa (SIS) when used for urinary bladder repair. Biomaterials 2001 Oct;22(19):2653–2659. [PubMed: 11519785]

27. Brennan EP, Reing J, Chew D, Myers-Irvin JM, Young EJ, Badylak SF. Antibacterial activity within degradation products of biological scaffolds composed of extracellular matrix. Tissue Eng 2006 Oct; 12(10):2949–2955. [PubMed: 17518662]

28. Li F, Li W, Johnson S, Ingram D, Yoder M, Badylak SF. Low-molecular-weight peptides derived from extracellular matrix as chemoattractants for primary endothelial cells. Endothelium 2004 May–Aug;11(3–4):199–206. [PubMed: 15370297]

29. Reing JE, Zhang L, Myers-Irvin J, Cordero KE, Freytes DO, Heber-Katz E, et al. Degradation products of extracellular matrix affect cell migration and proliferation. Tissue Eng Part A. 2008 Jul 24;

30. Sarikaya A, Record R, Wu CC, Tullius B, Badylak SF, Ladisch M. Antimicrobial activity associated with extracellular matrices. Tissue Eng 2002 Feb;8(1):63–71. [PubMed: 11886655]

31. Badylak SF, Park K, Peppas N, McCabe G, Yoder M. Marrow-derived cells populate scaffolds composed of xenogeneic extracellular matrix. Exp Hematol 2001 Nov;29(11):1310–1318. [PubMed: 11698127]

32. Zantop T, Gilbert TW, Yoder MC, Badylak SF. Extracellular matrix scaffolds are repopulated by bone marrow-derived cells in a mouse model of Achilles tendon reconstruction. J Orthop Res 2006 Jun;24(6):1299–1309. [PubMed: 16649228]

33. Beattie AJ, Gilbert TW, Guyot JP, Yates AJ, Badylak SF. Chemoattraction of progenitor cells by remodeling extracellular matrix scaffolds. Tissue Eng. 2008In Press

34. Freytes DO, Stoner RM, Badylak SF. Uniaxial and biaxial properties of terminally sterilized porcine urinary bladder matrix scaffolds. J Biomed Mater Res B Appl Biomater 2008 Feb;84(2):408–414. [PubMed: 17618508]

35. Freytes DO, Tullius RS, Badylak SF. Effect of storage upon material properties of lyophilized porcine extracellular matrix derived from the urinary bladder. J Biomed Mater Res B Appl Biomater 2006 Aug;78(2):327–333. [PubMed: 16365866]

36. Freytes DO, Tullius RS, Valentin JE, Stewart-Akers AM, Badylak SF. Hydrated versus lyophilized forms of porcine extracellular matrix derived from the urinary bladder. J Biomed Mater Res A. 2008 Jan 28;

37. Sacks MS. Incorporation of experimentally-derived fiber orientation into a structural constitutive model for planar collagenous tissues. J Biomech Eng 2003 Apr;125(2):280–287. [PubMed: 12751291]

38. Androjna C, Spragg RK, Derwin KA. Mechanical conditioning of cell-seeded small intestine submucosa: a potential tissue-engineering strategy for tendon repair. Tissue Eng 2007 Feb;13(2): 233–243. [PubMed: 17518560]

39. Gilbert TW, Stewart-Akers AM, Sydeski J, Nguyen TD, Badylak SF, Woo SL-Y. Gene expression by fibroblasts seeded on small intestinal submucosa and subjected to cyclic stretching. Tissue Eng 2007 Jun;13(6):1313–1323. [PubMed: 17518717]

40. Wallis MC, Yeger H, Cartwright L, Shou Z, Radisic M, Haig J, et al. Feasibility study of a novel urinary bladder bioreactor. Tissue Eng Part A 2008 Mar;14(3):339–348. [PubMed: 18333786]

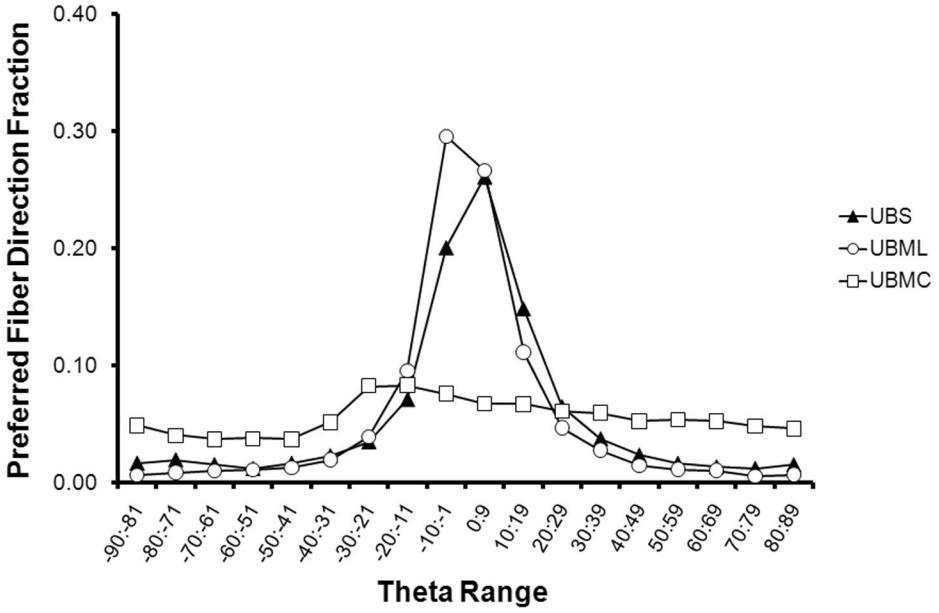

Figure 1.

A histogram of all measurements for each source of tissue shows a global preferred fiber orientation for UBML and UBS and a relatively homogenous distribution of collagen fibers for UBMC.

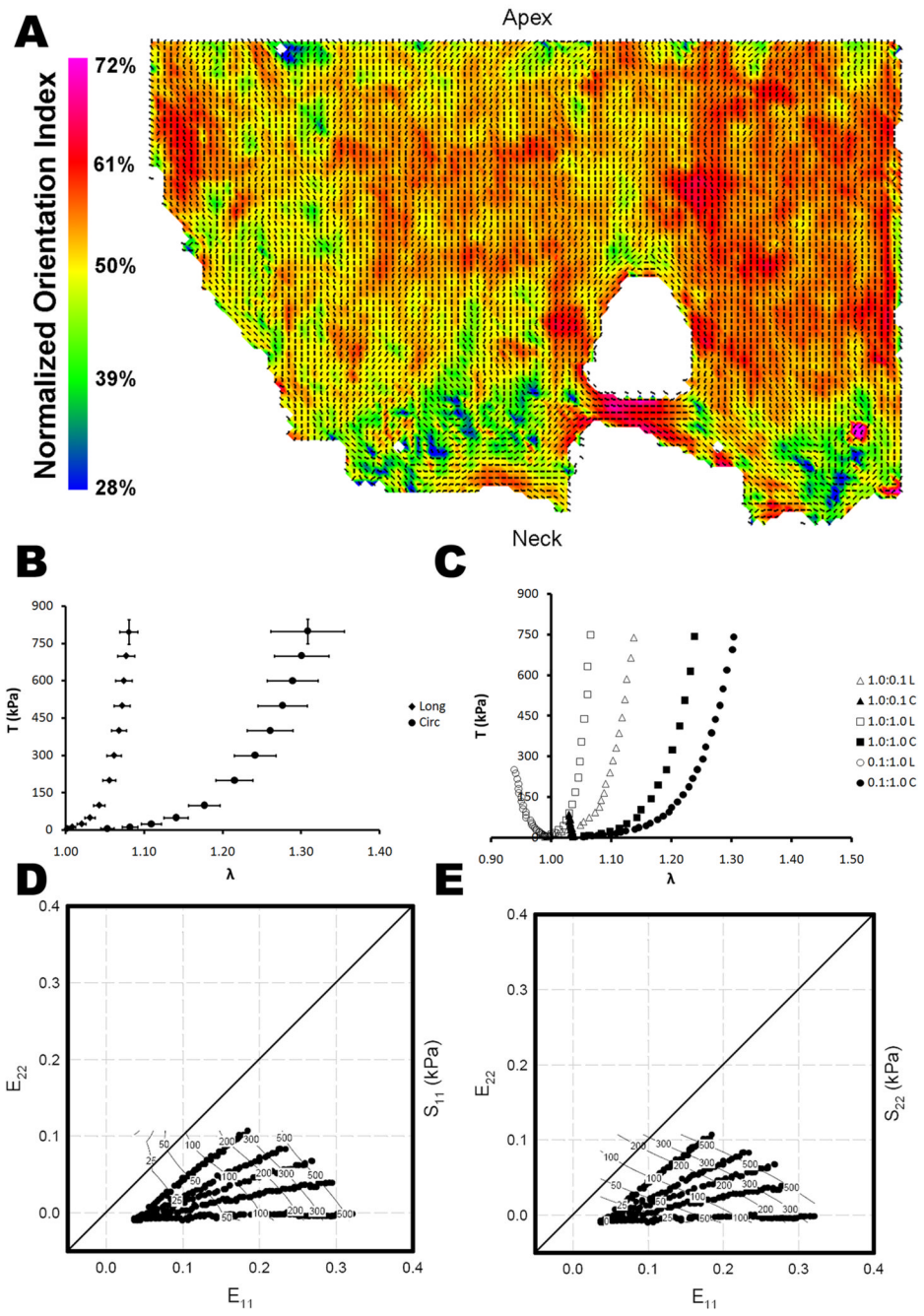

Figure 2.

(A) Representative collagen fiber orientation plots for urinary bladder matrix scraped longitudinally (UBML). The vectors indicate the local preferred fiber orientation and the color represents the normalized orientation index, a measure of the degree of alignment. (B) Average stress-strain relationship (mean ± standard error) for the longitudinal and circumferential axes of UBML for equibiaxial loading. (C) Representative stress-strain curves for three biaxial strain protocols for UBML. Representative stress contour plot for UBML in the (D) longitudinal direction and the (E) circumferential direction.

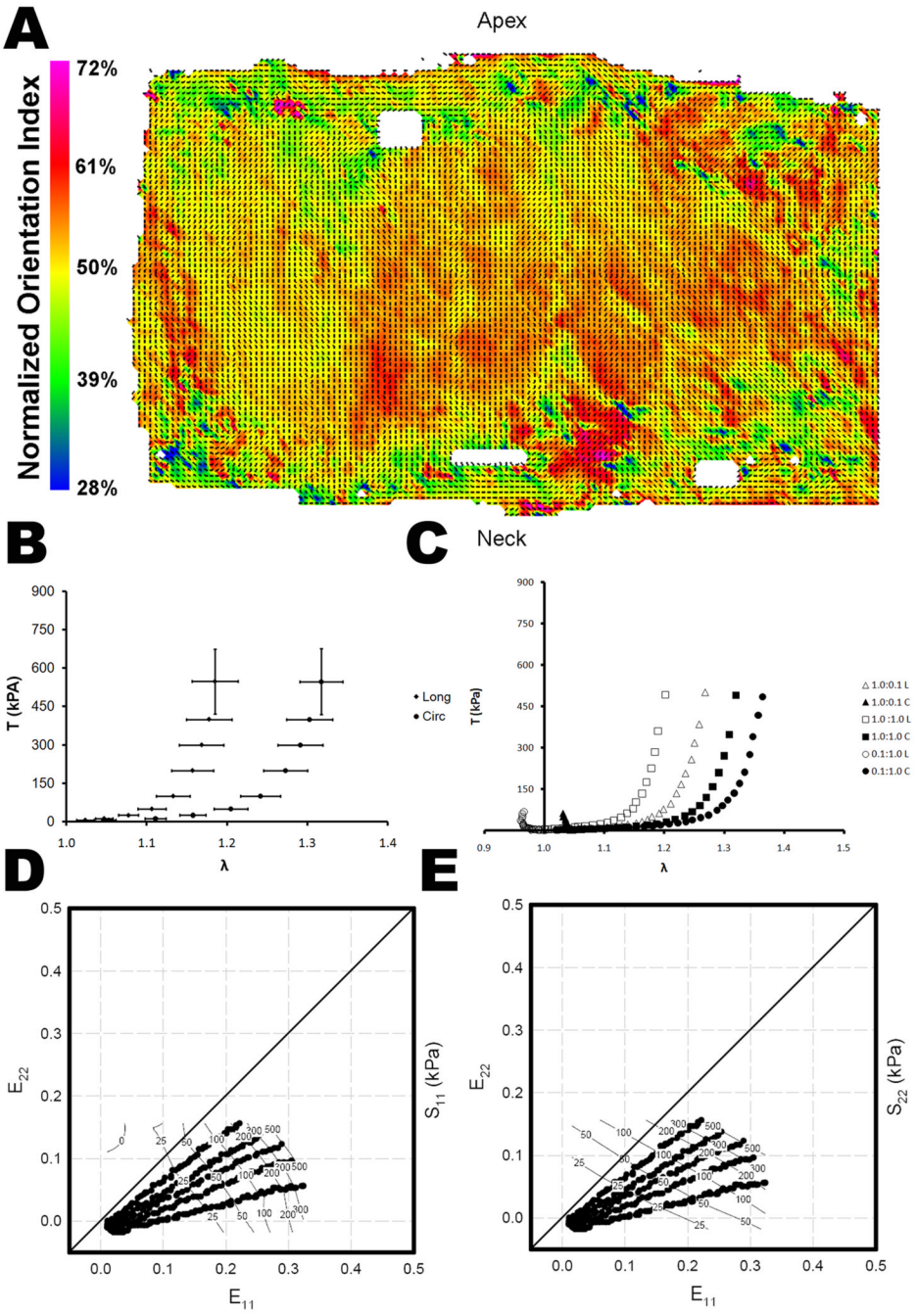

Figure 3.

(A) Representative collagen fiber orientation plots for urinary bladder submucosa (UBS). The vectors indicate the local preferred fiber orientation and the color represents the normalized orientation index, a measure of the degree of alignment. (B) Average stress-strain relationship (mean ± standard error) for the longitudinal and circumferential axes of UBS for equibiaxial loading. (C) Representative stress-strain curves for three biaxial strain protocols for UBS. Representative stress contour plot for UBS in the (D) longitudinal direction and the (E) circumferential direction.

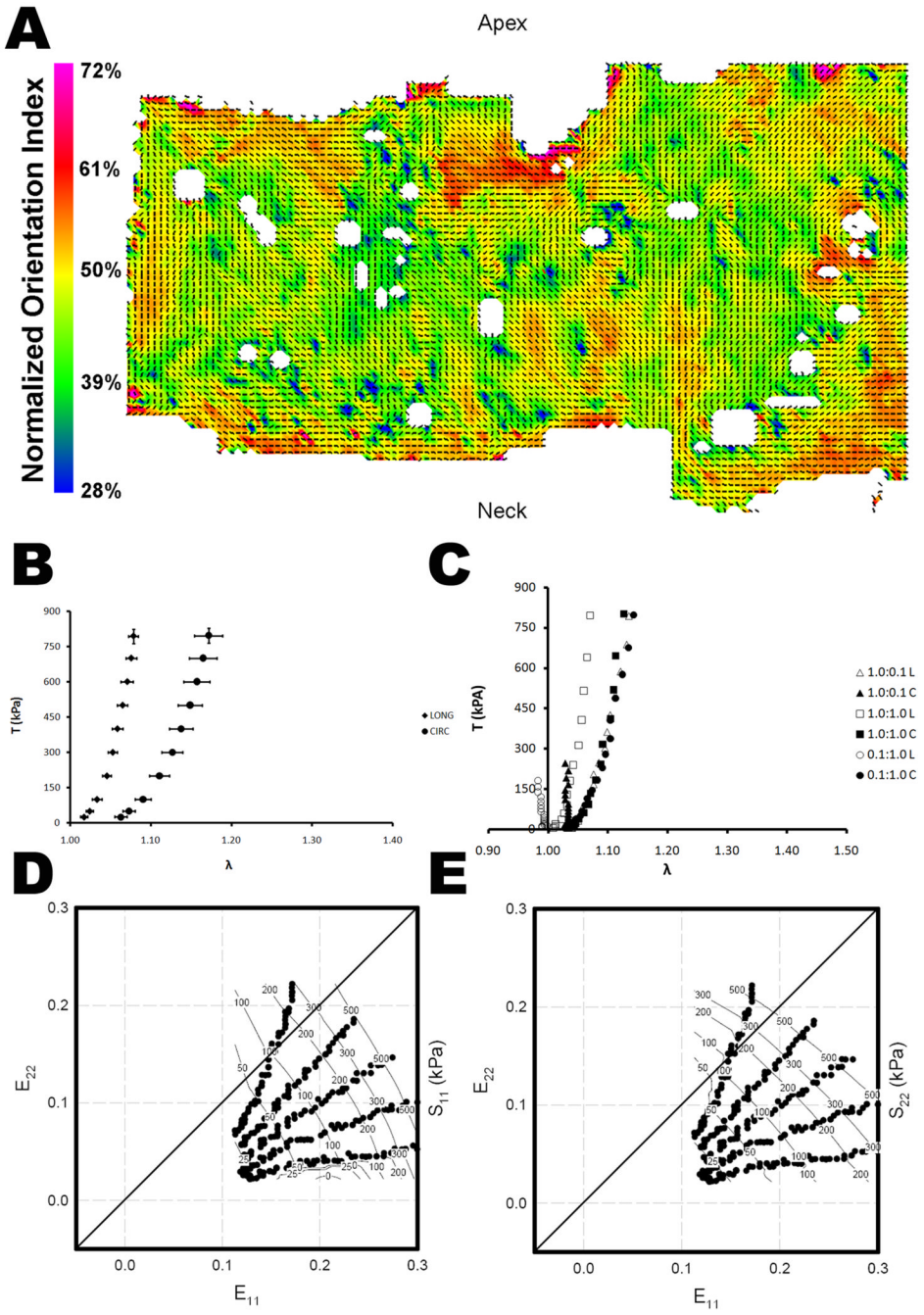

Figure 4.

(A) Representative collagen fiber orientation plots for urinary bladder matrix scraped circumferentially (UBMC). The vectors indicate the local preferred fiber orientation and the color represents the normalized orientation index, a measure of the degree of alignment. (B) Average stress-strain relationship (mean ± standard error) for the longitudinal and circumferential axes of UBMC for equibiaxial loading. (C) Representative stress-strain curves for three biaxial strain protocols for UBMC. Representative stress contour plot for UBMC in the (D) longitudinal direction and the (E) circumferential direction.

Table 1

Modulus and stretch in toe region for equibiaxial mechanical testing of UBML, UBMC, and UBS.

	Modulus (MPa)		Stretch in Toe Region	
	Longitudinal Direction	**Circumferential Direction**	**Longitudinal Direction**	**Circumferential Direction**
UBML	25.9 ± 10.6*	4.7 ± 2.0	1.04 ± 0.02§	1.18 ± 0.04
UBMC	17.6 ± 4.8*	6.9 ± 1.1	1.03 ± 0.01§	1.09 ± 0.02†
UBS	10.4 ± 3.2*†	9.6 ± 2.0†	1.13 ± 0.05§†	1.24 ± 0.06

*Statistically greater than circumferential direction;

§Statistically less than circumferential direction;

†Statistically different from other scaffolds in the same direction of measurement ($p < 0.05$).